Annals of Case Reports
Boutary S, et al. Ann Case Rep: 11: 102596
www.doi.org/10.29011/2574-7754.102596
www.gavinpublishers.com

OPEN ACCESS

GAVIN PUBLISHERS

Case Study

Sustained Therapeutic Efficacy of siPMP22-Squalene Nanoparticles in the C61 Mouse Model of CMT1A: A Preclinical Case Study for Clinical Translation

Suzan Boutary[1], Elena-Gaia Banchi[2], Françoise Piguet[2], Liliane Massaad-Massade[1*]

[1]U1195 Diseases and Hormones of the Nervous System, Inserm and University Paris-Saclay, 94276 Le Kremlin-Bicêtre, France

[2]Innovation Unit GENOV, Paris Brain Institute, Inserm U 1127, CNRS UMR 7225, Sorbonne Université, F-75013 Paris, France

[*]**Corresponding author**: Liliane Massaad-Massade, U1195 Diseases and Hormones of the Nervous System, Inserm and University Paris-Saclay, 94276 Le Kremlin-Bicêtre, France

Citation: Boutary S, Banchi EG, Piguet F, Massaad-Massade L. (2026). Sustained Therapeutic Efficacy of siPMP22-Squalene Nanoparticles in the C61 Mouse Model of CMT1A: A Preclinical Case Study for Clinical Translation. Ann Case Report. 11: 2596. DOI: 10.29011/2574-7754.102596

Received: 10 April 2026; **Accepted:** 16 April 2026; **Published:** 20 April 2026

Abstract

Charcot-Marie-Tooth disease type 1A (CMT1A) results from PMP22 gene duplication, leading to chronic demyelination and progressive peripheral neuropathy. We previously showed that systemic delivery of squalene-conjugated siRNA nanoparticles (siRNA PMP22-SQ NPs) improves motor function in C61 transgenic mice. Here, we investigated the durability and dose-dependence of this nanomedicine-based RNA interference approach. In one-month-old C61 mice, a cumulative dose of 1.5 mg/kg induced rapid improvement of locomotion, grip strength, and compound muscle action potentials (CMAPs), with functional benefits lasting approximately 28 days. Repeated treatment cycles-maintained motor improvement for more than 100 days. Reducing the cumulative dose five-fold (0.3 mg/kg) in two-month-old mice produced a prolonged functional improvement lasting approximately 100 days, and a second cycle restored motor performance after relapse. Western blot analysis showed no significant change in total PMP22 protein levels at 1.5 mg/kg, whereas treatment at 0.3 mg/kg selectively reduced aberrant PMP22 species while preserving the mature glycosylated form. Morphometric g-ratio analysis revealed pronounced axon-myelin remodeling at the lower dose, consistent with preferential remyelination rather than complete normalization to wild-type values. Serum biochemistry and histopathological analyses revealed no detectable systemic toxicity at either dose. Overall, these results demonstrate that low-dose systemic administration of siRNA PMP22-SQ nanoparticles induces durable and repeatable recovery of motor function with a favorable safety profile. Importantly, functional improvement is accompanied by structural remodeling of axon–myelin units, supporting sustained nerve repair rather than transient compensation. These findings provide preclinical evidence supporting the therapeutic potential of squalene-based siRNA nanomedicines for CMT1A.

Keywords: C61 CMT1A mouse model; siRNA PMP22-squalene nanoparticles; Gene silencing; Long-lasting therapeutic effect; Safety profile

Introduction

Charcot-Marie-Tooth disease type 1A (CMT1A) is the most prevalent inherited demyelinating neuropathy, accounting for approximately 70% of all CMT cases. It results from a 1.4 Mb duplication on chromosome 17p11.2 encompassing the Peripheral Myelin Protein 22 (PMP22) gene [1]. The ensuing 1.5-fold PMP22 overexpression disrupts Schwann cell homeostasis, leading to myelin instability, axonal degeneration, and progressive muscle weakness [2]. Despite extensive efforts and the recent phase III evaluation of the fixed-dose combination PXT3003 [3], no approved disease-modifying therapy is currently available, and treatment remains largely supportive [4].

Because the disease mechanism is gene-dosage dependent, therapeutic strategies have focused on normalizing PMP22 expression through gene silencing or transcriptional regulation. Several approaches, including antisense oligonucleotides, siRNA, and miRNA-based AAV vectors, have demonstrated proof of concept efficacy in preclinical models [5-8]. Among these, RNA interference targeting PMP22 has emerged as a particularly promising approach, as transient downregulation is sufficient to restore myelination and improve nerve conduction in rodent and in non-human primate models [4, 9].

We previously developed a squalene-based siRNA delivery platform, in which conjugation of siRNA to a biocompatible squalene moiety enables spontaneous nanoparticle self-assembly, efficient systemic delivery, and accumulation in peripheral nerves without viral vectors [10-12]. Using this system, we showed that siRNA PMP22-SQ nanoparticles (siRNA PMP22-SQ NPs) at 1.5 mg/kg restored locomotor and electrophysiological functions in C61 transgenic mice, a CMT1A mouse model [9].

However, critical questions remain unresolved regarding the durability of therapeutic benefit, the minimal effective dose required for long-term correction, and the feasibility of repeated systemic administration without loss of efficacy or safety. In particular, it is unknown whether transient PMP22 silencing can induce sustained functional and structural recovery after treatment cessation, or whether repeated treatment cycles remain effective as disease progresses.

Here, we evaluated the long-term efficacy of siRNA PMP22-SQ NPs and the persistence of therapeutic benefit after repeated treatment cycles and determined whether similar improvements could be achieved at a five-fold lower cumulative dose (0.3 mg/kg). In our previous therapeutic studies targeting papillary thyroid carcinoma and prostate cancer, repeated administration of lower, fractionated doses of siRNA-squalene NPs were sufficient to induce sustained gene silencing and significantly reduce tumor burden while minimizing systemic toxicity [13, 14]. Based on this evidence, we hypothesized that reduced cumulative doses could similarly provide prolonged therapeutic benefit in CMT1A without compromising safety.

We further sought to delineate the molecular correlates of recovery, focusing on PMP22 expression and myelin integrity, and to assess the safety and tolerability of repeated systemic administration. By comparing early versus late treatment initiation and high versus low dosing, this study establishes, for the first time, the durability, repeatability, and safety of systemic siRNA-mediated PMP22 silencing, thereby strengthening the translational potential of RNA interference-based therapies for CMT1A.

Materials and Methods

Chemicals

All chemicals were of analytical grade and were used as received. Modified siRNAs used for copper-free click chemistry were purchased from Eurogentec (France). Azido-squalene and cationic squalene were synthesized by Dr. Didier Desmaële (Galien Institute, Université Paris-Saclay) according to previously published procedures.

For nanoparticle formulation and buffer preparation, Tris (hydroxymethyl) aminomethane (Tris), sodium chloride (NaCl), ethylenediaminetetraacetic acid (EDTA), magnesium acetate, potassium acetate, and HEPES-KOH (pH 7.4) were purchased from Sigma-Aldrich. Acetone (HPLC grade) used during the conjugation and purification steps was obtained from Sigma-Aldrich.

For in vivo studies, D-glucose formulated as a 5% (w/v) dextrose solution was used as vehicle control. For protein analyses, RIPA buffer supplemented with a protease inhibitor cocktail (Sigma-Aldrich) was used for tissue lysis. Bradford reagent and Clarity™ Western ECL substrate were purchased from Bio-Rad. Sodium dodecyl sulfate (SDS) and all reagents used for SDS-PAGE and immunoblotting were of analytical grade.

For histological and morphological analyses, toluidine blue O was used for staining semi-thin sciatic nerve sections, and hematoxylin and eosin Y were used for hematoxylin-eosin staining of paraffin-embedded tissues. All reagents were used according to the manufacturers' instructions

Preparation of siRNA-Squalene Nanoparticles

The synthesis and formulation of siRNA PMP22-SQ NPs and control siRNA-SQ NPs were performed exactly as previously described [4, 9]. Briefly, DBCO-siRNA and N_3-squalene were

conjugated by copper-free click chemistry, followed by purification by HPLC and inverse nanoprecipitation. Equimolar hybridization of sense siRNA-SQ and antisense strands generated stable duplexes. Physicochemical characteristics (size, PDI, ζ-potential) were routinely verified by dynamic light scattering (DLS) and Nanodrop spectrophotometry prior to use.

Animal Model, Experimental Design, and Objectives

Experiments were conducted in C61 transgenic mice (4 copies of human PMP22, C57BL/6J background) [15, 16] and WT littermates were used. Both sexes included, aged 1-2 months, weighing 18-24 g. Mice were housed in groups of 3-5 per cage under 12 h light/dark, 22 ± 2°C, 50 ± 10% humidity, with environmental enrichment. Animal housing, anesthesia, and euthanasia procedures complied with EU Directive 2010/63/EU and were approved by the French MESR Ethics Committee (APAFIS #44312-2023042616547465). All studies adhered to the 3Rs principle and groups were balanced for sex and age.

Three complementary experimental protocols with randomized group assignment and blinding of outcome assessments were performed to evaluate the therapeutic potential of siRNA PMP22-SQ NPs in C61 mice, each addressing a specific objective. Both male and female mice were included, balanced across experimental groups. No sex-dependent differences were observed, and data were therefore pooled.

Experiment 1: early intervention and long-term persistence

One-month old animals received three intravenous injections of 0.5 mg/kg siRNA PMP22-SQ NPs or 5% dextrose (vehicle) at three-day intervals (first cycle). Age-matched WT mice served as untreated controls (n = 3). Behavioral and electrophysiological assessments were performed bi-weekly. Upon relapse, a second and subsequently a third identical treatment cycle were administered. After completion of the final cycle, mice were sacrificed at 8.4 months. Sciatic nerves were collected for semi-thin morphological analysis and Western blot quantification of PMP22 expression. Blood and major organs (liver, kidney, heart, spleen, lung, brain, and spinal cord) were harvested for biochemical assays and morphological examination.

Experiment 2: low dose efficacy

Eight-week-old C61 mice received three intravenous injections of 0.1 mg/kg siRNA PMP22-SQ NPs (n = 5), control siRNA-SQ NPs (n = 5), or 5% dextrose (n = 5) at three-day intervals. Age-matched WT mice were used as physiological reference controls (n = 5). Behavioral and CMAP measurements were performed before and after treatment. Mice were sacrificed after the final evaluations.

Experiment 3: durability of low-dose treatment

Eight-week-old C61 mice received the same low-dose regimen (0.1 mg/kg × 3; cumulative dose 0.3 mg/kg; n = 3) or 5% dextrose (n = 3) and were monitored for 140 days post-treatment. Age matched WT mice were included as stable physiological controls (n = 3). Behavioral and CMAP tests were performed biweekly, and a second treatment cycle was administered upon relapse (~100 days after the first injection). After completion of the final evaluations, mice were sacrificed. Sciatic nerves, blood, and major organs were collected for morphological, biochemical, and safety assessments.

Mice were randomly assigned to treatment groups. Behavioral, electrophysiological, and histopathological analyses were performed. No animals were excluded unless they presented unrelated health issues or technical artifacts, and all exclusion events were documented. Animals were monitored daily by certified personnel for posture, gait, hydration status, and signs of discomfort. Humane endpoints were predefined according to EU regulations.

Behavioral and Electrophysiological Analyses

Beam walking, Locotronic, and grip strength assessments were performed and scored by a blinded observer, as previously described [4, 9]. Compound muscle action potential (CMAP) recordings were acquired and analyzed in a blinded manner using a Natus UltraPro S100 EMG system, in accordance with AANEM guidelines, with constant electrode placement, pulse duration (0.1 ms), and stimulation intensity parameters, as previously reported [4, 9].

Histological and Biochemical Analyses

Procedures for sciatic nerve fixation, embedding, and toluidine blue staining followed established protocols [4] For systemic toxicity evaluation, H&E staining of major organs was performed by Excilone SAS and reviewed by a board-certified pathologist blinded to treatment allocation (Dr. C. Adam, Hôpital Kremlin-Bicêtre). Serum biomarkers (ALP, ALT, AST, HDL, LDL, total cholesterol, LDH, albumin, bilirubin, creatinine) were quantified on a Pentra 400 analyzer (Enterosys/Prologue Biotech) as described [9].

g-Ratio Analysis

Semi-thin sections were stained with toluidine blue and scanned via blinded automated software at 40× magnification using a NanoZoomer S60 slide scanner (Hamamatsu, France). Images were analyzed using Visiopharm software (version 2025.02). Axons and myelin sheaths were segmented by an algorithm generated using a deep learning U-Net architecture trained on nine manually annotated images.

Western Blot

Protein extraction and immunoblotting procedures were performed as described [9]. Briefly, sciatic nerves were homogenized in RIPA buffer supplemented with protease inhibitors, and 5 µg total protein per sample was resolved on 8-12% SDS-PAGE, transferred to nitrocellulose membranes, and probed with anti-PMP22 (ab270400, abcam Supplier, 1:1000) and anti-tubulin antibodies (EPR13797, Abcam, 1:3000). Detection was performed using HRP-conjugated secondary antibodies and enhanced chemiluminescence. Densitometric analysis was performed using a Python-based image analysis pipeline equivalent to ImageJ. Band intensities were quantified by pixel density integration after background subtraction using fixed molecular-weight windows corresponding to PMP22 isoforms (~24, ~22 and ~18 kDa). Total PMP22 intensity was calculated by summing the intensity of each individual isoform. Wild-type samples served as the biological reference for relative quantification. PMP22 signals were then normalized to tubulin and expressed relative to WT values.

Statistics

Statistical analyses were performed using GraphPad Prism (version 10.4.1). Normality of data distribution was assessed prior to statistical testing. For longitudinal behavioral and electrophysiological experiments involving comparisons between wild-type and treated C61 groups, data were normalized relative to wild-type values at each corresponding time point. Then, statistical significance between experimental groups was assessed at each time point using the non-parametric Mann–Whitney test with false discovery rate (FDR) correction. For experiments comparing multiple treatment groups at a single endpoint, parametric datasets were analyzed using one-way analysis of variance (ANOVA) followed by Tukey's multiple comparisons test. For morphometric analyses, including g-ratio measurements, non-parametric comparisons were performed using the Kruskal-Wallis test, as appropriate. A large number of nerve fibers per animal were quantified, providing robust within-animal sampling. Outliers were identified using Grubbs' test. The individual animal was considered the experimental unit. Data are presented as mean ± SD. A p-value < 0.05 was considered statistically significant.

Results

Long term and age dependent effects of siRNA PMP22-SQ nanoparticles (1.5 mg/kg)

We previously demonstrated that a cumulative dose of 1.5 mg/kg of siRNA PMP22-SQ NPs restores motor and electrophysiological performance in C61 CMT1A mice [9]. Previously Stavrou et al. [8] showed that treatment at early and late stages of the disease significantly improved multiple functional outcome measures [8]. Here, we extended this work to evaluate the durability and age dependence of the therapeutic effect after multiple treatment cycles (Figure 1A). Therefore, one month old C61 mice received three intravenous injections of 0.5 mg/kg each (1.5 mg/kg cumulative dose), followed by behavioral and electrophysiological follow-up for up to eight months. After the first treatment cycle, locomotion and grip strength were rapidly restored and remained significantly improved for approximately 29 days (Figure 1B-E). A second treatment cycle administered at 68 days (~9 weeks) maintained normalized locomotor performance and CMAP amplitude up to 110 days (corresponding to 23 weeks of mice age) (Figure 1F). A third treatment cycle was then performed and led to a transient re-establishment of functional improvement lasting approximately 100 days (over three months), indicating that re-treatment remains effective even in older animals. Western blot analysis of sciatic nerve lysates revealed a marked increase in overall PMP22 protein levels in C61 transgenic mice compared with wild-type (WT) controls (Figure 1G). Semi-quantitative densitometric analysis normalized to tubulin indicated an approximately four-fold elevation of total PMP22 expression in C61 nerves, consistent with PMP22 gene quadruplication. At the tested dose (1.5 mg/kg), treatment with siRNA PMP22-SQ NPs did not result in a statistically significant change in total PMP22 protein levels compared with untreated C61 mice (Figure 1H). Further examination of PMP22 immunoreactive species revealed three bands migrating at approximately 24, 22, and 18 kDa, corresponding respectively to the mature glycosylated form (complex Golgi), the immature high-mannose form retained in the endoplasmic reticulum, and the non-glycosylated core protein as previously described [17-19]. Semi-quantitative assessment of isoform distribution showed that WT mice predominantly expressed the glycosylated and mature forms with relatively balanced proportions, whereas C61 transgenic mice displayed a marked predominance of the 22 kDa band, with low or undetectable levels of the glycosylated form and a variable expression of the 18 kDa species. Following treatment with siRNA PMP22-SQ NPs (1.5 mg/kg), isoform distribution remained largely comparable to those observed in untreated C61 mice, although one treated animal exhibited detectable levels of all three isoforms. Given the semi-quantitative nature of this analysis and the inter-individual variability observed, these data are presented in Figure 2.

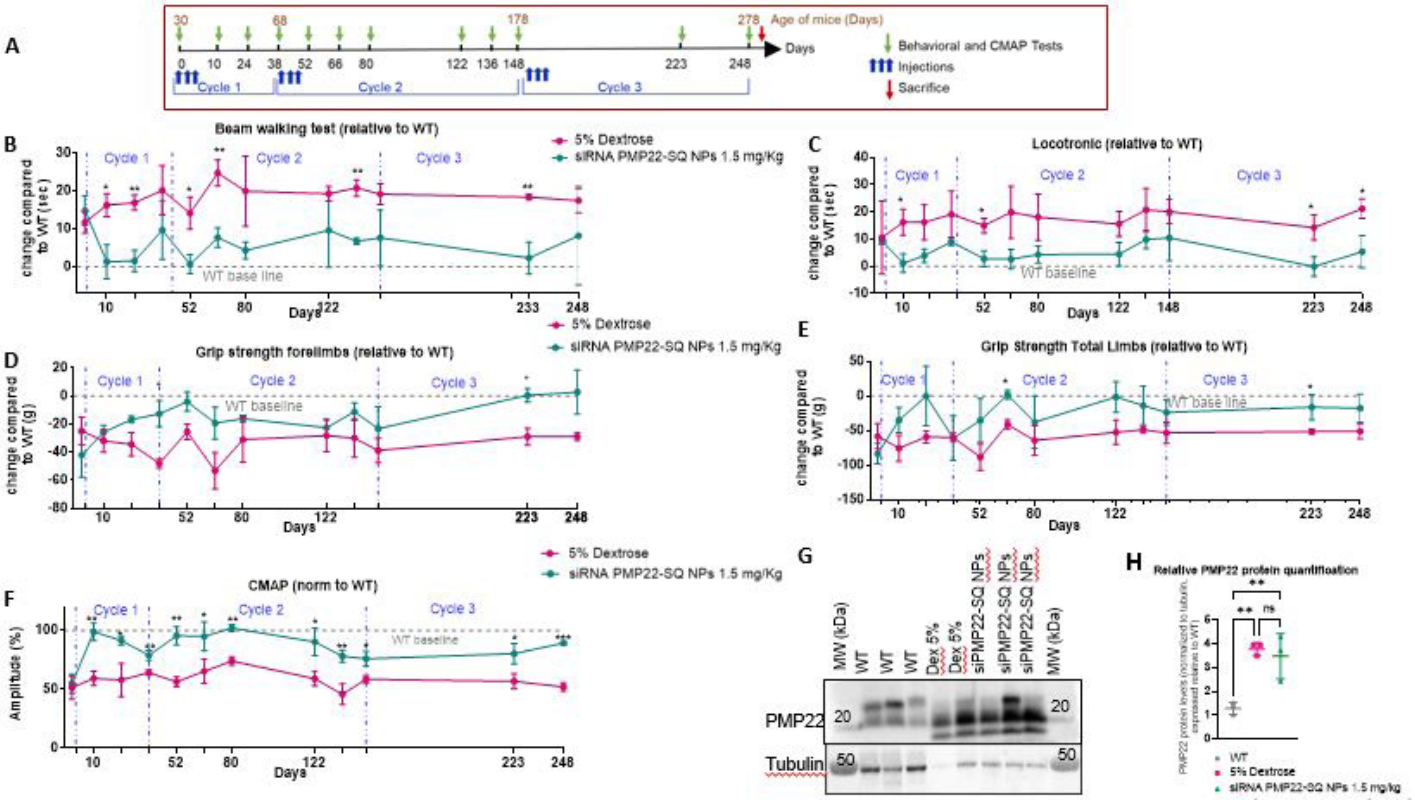

Figure 1 : Long-term and age-dependent effects of siRNA PMP22-SQ nanoparticles (1.5 mg/kg) in C61 CMT1A mice. (A) Experimental timeline illustrating treatment cycles, injection schedules, behavioral and CMAP assessments, and sacrifice time points. **(B-F)** Longitudinal analysis of behavioral and electrophysiological outcomes measured across three treatment cycles and expressed relative to wild-type (WT) baseline values. Behavioral tests were performed before each treatment cycle and 3 days and every 2 weeks after the end of treatment, as shown in **(B-E).** Behavioral data are displayed as relative differences compared with wild-type mice at each time point, such that the dotted line at y = 0 represents the average wild-type value. CMAP recordings were performed immediately after the first treatment cycle and every 2 weeks thereafter, as shown in **(F).** Three animals per group were analyzed for each test and followed for a period of 8 months. Data are presented as mean ± SD. Statistical significance was assessed using the Mann–Whitney non-parametric test at each time point between the two experimental groups, with false discovery rate (FDR) correction (*$p < 0.05$; **$p < 0.01$; ***$p < 0.001$). **(G)** Representative Western blot showing PMP22 protein expression in sciatic nerves, with tubulin used as a loading control. **(H)** Densitometric quantification of PMP22 band intensities were quantified, normalized to tubulin, and expressed relative to WT values. Statistical significance is indicated ($p < 0.01$; ns, not significant).

A

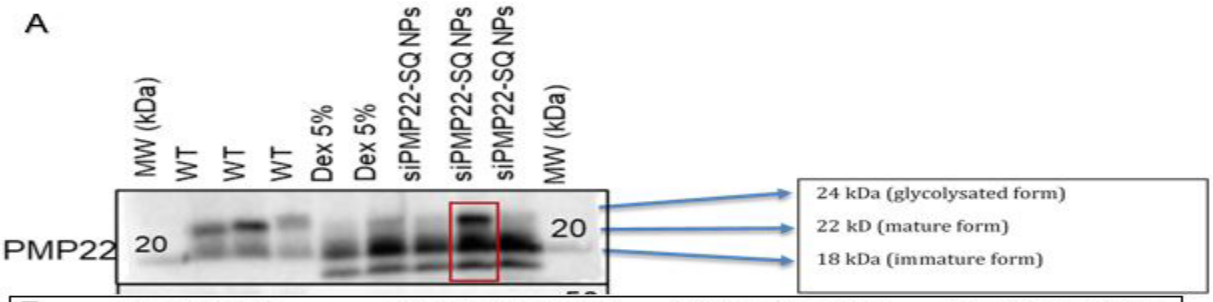

B

Conditions	24 kDa (a.u.) (%)	22 kDa (a.u.) (%)	18 kDa (a.u.) (%)
WT	5271 (71%)	2131 (29%)	0
WT	9508 (69%)	4152 (31%)	0
WT	2490 (52%)	2312 (48%)	0
5% Dextrose	0	11445 (86%)	1894(14%)
5% Dextrose	0	22605 (97%)	542 (3%)
siRNA PMP22-SQ NPs (1.5 mg/kg)	0	19951 (94%)	1218.8 (6%)
siRNA PMP22-SQ NPs (1.5 mg/kg)	6964 (37%)	9632 (50%)	2379 (13%)
siRNA PMP22-SQ NPs (1.5 mg/kg)	0	24223 (96%)	947(4%)

Figure 2. PMP22 isoform expression and densitometric quantification in sciatic nerves: treatment at 1.5 mg/kg (cumulative dose). **A**. PMP22 is detected as three distinct bands corresponding to the fully glycosylated form (~24 kDa), the mature form (~22 kDa), and the immature/non-glycosylated form (~18 kDa), as indicated. The red box highlights the condition in which all three PMP22 isoforms are simultaneously detected. **B**. Densitometric analysis was performed by integrating the pixel intensity of each individual band. For each sample, isoform distribution is expressed as absolute intensity (a.u.) and as a percentage of total detected PMP22 signal, with percentages summing to 100% per lane. WT samples predominantly display the 24 kDa and 22 kDa isoforms, whereas 5% dextrose–treated samples mainly show the 22 kDa and 18 kDa forms. Treatment with siRNA PMP22-SQ NPs (1.5 mg/kg) results in a redistribution of PMP22 isoforms, with the appearance of all three forms in one sample, suggesting a partial restoration of PMP22 maturation.

Efficiency of siRNA PMP22-SQ nanoparticles at a five-fold lower dose (0.3 mg/kg)

To determine whether lower doses could achieve comparable efficacy, two-month-old C61 mice were treated with a cumulative dose of 0.3 mg/kg (three intravenous injections of 0.1 mg/kg) or with control formulations (vehicle or siRNA CTRL-SQ NPs) (Figure 3A). Interestingly, all treated mice exhibited a rapid and significant improvement in locomotor performance in the beam-walking and locotronic tests compared with control groups (Figure 3B-C). Muscle strength increased in both forelimbs and hind limbs (Figure 3D-E), and CMAP amplitudes were restored to wild type levels (Figure 3F).

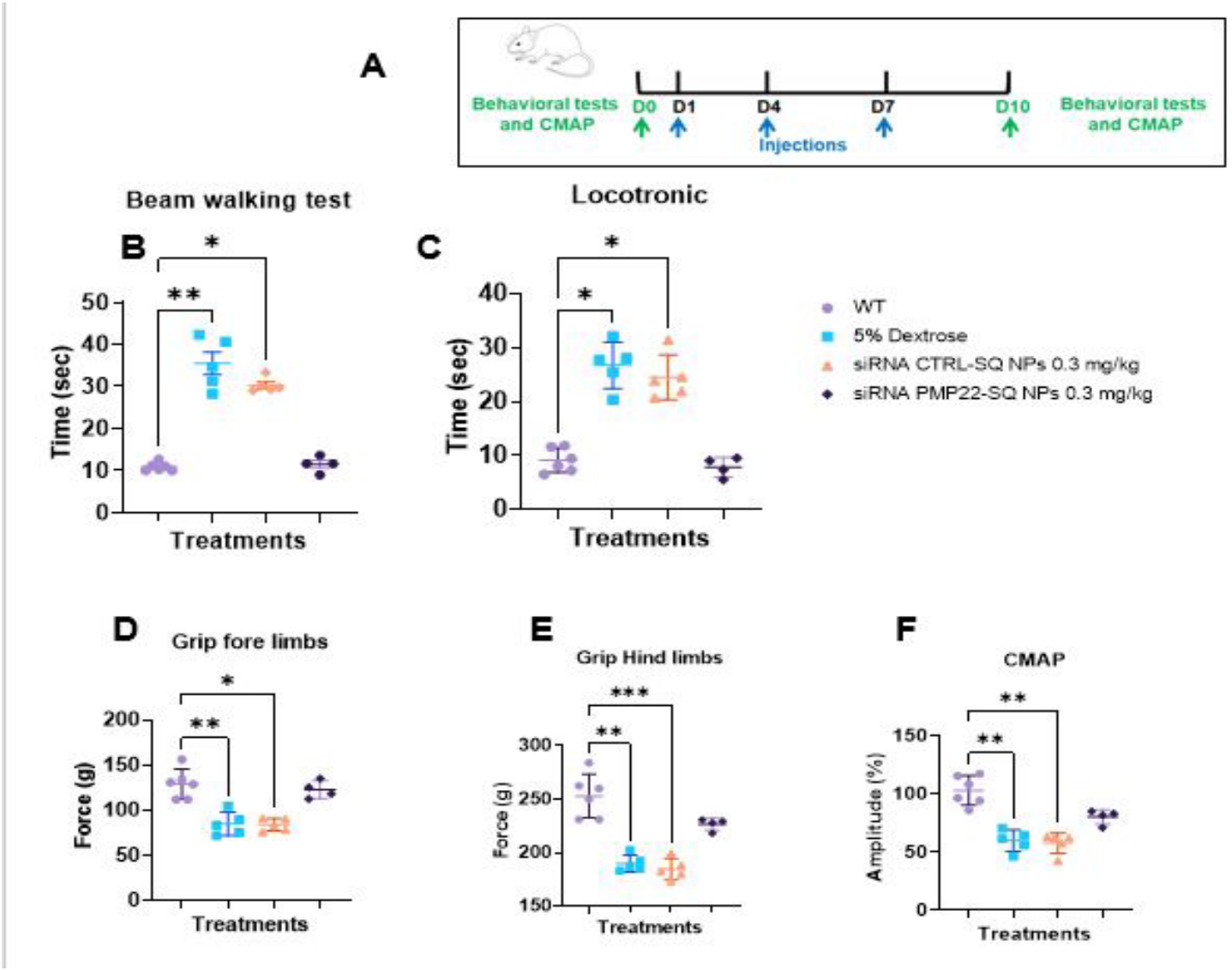

Figure 3: Functional efficacy of siRNA PMP22-SQ nanoparticles at a low cumulative dose (0.1 mg/kg × 3). **(A)** Experimental scheme showing three intravenous injections administered at 3-day intervals and sacrifice at day 10 (D10). (**B-E)** Behavioral outcomes assessed at D10, including beam-walking performance, Locotronic test, and forelimb and hind limb grip strength. **(F)** CMAP amplitudes recorded from the sciatic nerve. Each dot represents one animal (n = 4-5 per group). Data are presented as mean ± SD. Statistical analysis was performed using one-way ANOVA followed by Tukey's multiple comparisons test *p < 0.05; **p < 0.01; ***p < 0.0001.

Long-lasting effects of repeated low-dose siRNA PMP22-SQ NP treatment in C61 CMT1A mice.

Two-month-old C61 mice were intravenously treated with siRNA PMP22-SQ NPs at a cumulative dose of 0.3 mg/kg (Figure 4A). Following treatment, locomotor performance, grip strength and CMAP amplitudes were rapidly improved and remained significantly enhanced for nearly 100 days. Upon relapse at ~6 months of age, a second identical treatment cycle again restored motor performance and CMAP amplitudes to near WT levels, confirming the durability and reproducibility of the therapeutic effect (Figure 4B-F). At the terminal endpoint, approximately 100 days after the second treatment cycle and following completion of behavioral and electrophysiological assessments, mice were sacrificed at 9.2 months and sciatic nerves were collected for biochemical and histological analyses. Western

blot analysis of sciatic nerve extracts revealed that, in contrast to the higher dose (1.5 mg/kg), treatment at 0.3 mg/kg resulted in an apparent normalization of PMP22 protein levels (Figure 4 G-H, Figure 5). This effect was driven, in two out of three animals, by a marked reduction of both 22 kDa and 18 kDa PMP22 isoforms, while the 24 kDa glycosylated form was preserved, consistent with partial restoration of PMP22 proteostasis (Figure 6).

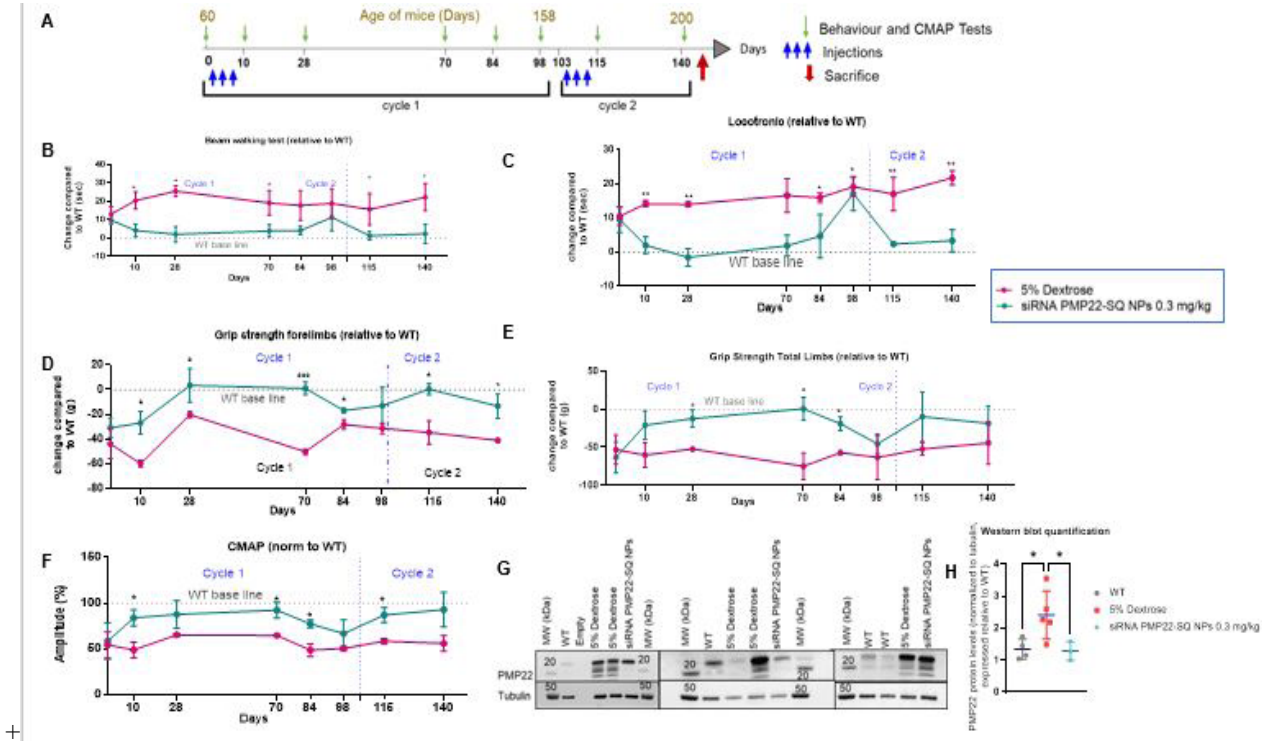

Figure 4: Long-lasting effects of repeated low dose siRNA PMP22-SQ NP treatment in C61 CMT1A mice. (A) Experimental design. Two-month-old C61 mice received two treatment cycles of siRNA PMP22-SQ NPs (three intravenous injections of 0.1 mg/kg, administered every 3 days; cumulative dose of 0.3 mg/kg per cycle). Behavioral assessments (beam walking, Locotronic ladder and grip strength) and CMAP recordings were performed before treatment, 3 days after the last injection of each cycle, and then approximately every two weeks until relapse. Mice were sacrificed at 6.7 months of age for molecular and histological analyses. (B-C) Beam-walking and Locotronic ladder performance expressed relative to WT baseline. siRNA PMP22-SQ NP–treated mice showed sustained functional improvement after each treatment cycle, whereas 5% dextrose–treated C61 mice remained impaired. (D-E) Forelimb and total limb grip strength expressed relative to WT baseline progressively improved following siRNA PMP22-SQ NP treatment, approaching WT levels after each cycle. (F) Sciatic nerve CMAP amplitudes normalized to WT baseline, showing recovery after each treatment cycle followed by a gradual decline prior to retreatment. Statistical significance was assessed using the Mann–Whitney non parametric test at each time point between the two experimental groups, with false discovery rate (FDR) correction (*$p < 0.05$; * *$p < 0.01$; ***$p < 0.001$). (G) Western blot analysis of sciatic nerve extracts showing PMP22 immunoreactive bands. (H). PMP22 band intensities were quantified, normalized to tubulin, and expressed relative to WT values. A reduction of the aberrant 22 kDa and 18 kDa PMP22 forms was observed in two out of three siRNA PMP22-SQ NP-treated mice, while the 24 kDa glycosylated form was preserved. α-Tubulin served as a loading control. (*$p < 0.05$).

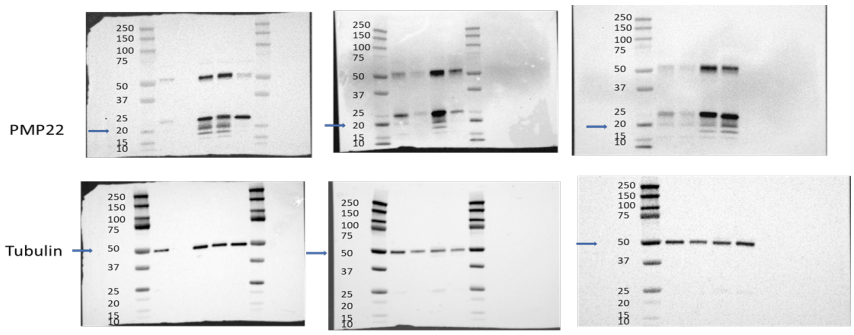

Figure 5: Uncropped Western blot membranes corresponding to the cropped blots shown in Figure 3H. Three independent Western blot experiments were performed. Uncropped membranes for PMP22 (upper panel) and tubulin (lower panel) are shown. Precision Plus Protein™ Dual Color Standards (Bio-Rad) were used as molecular weight markers. Lanes are presented in the same order as in the corresponding main Figure 4.

A

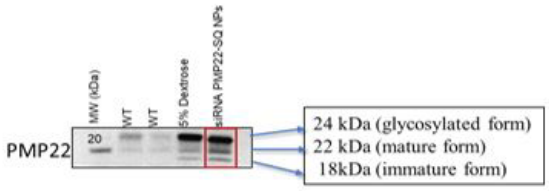

B.

Conditions	24 kDa (a.u.) (%)	22 kDa (a.u.) (%)	18 kDa (a.u.) (%)
WT	399229 (67%)	197387 (33%)	0.0
WT	2575154 (100%)	0	0
WT	910490 (75%)	306158 (25%)	0
WT	1358027 (52%)	1262597 (48%)	0
5% Dextrose	2339739 (50%)	1583596 (34%)	782704 (16%)
5% Dextrose	2365294 (53%)	1432240 (32%)	657490 (15%)
5% Dextrose	289157 (100%)	0	0
5% Dextrose	1780000 (83%)	920000 (33%)	110000 (4%)
5% Dextrose	1780000 (83%)	920000 (33%)	110000 (4%)
siRNA PMP22-SQ NPs (0,3 mg/kg)	2605778 (100%)	0.0	0.0
siRNA PMP22-SQ NPs (0,3 mg/kg)	662606 (100%)	0	0
siRNA PMP22-SQ NPs (0,3 mg/kg)	601133 (41%)	536145 (37%)	319901 (22%)

Figure 6: Isoform distribution in sciatic nerves following siRNA PMP22-SQ NPs treatment (0.3 mg/kg). A). PMP22 is detected as three distinct bands corresponding to the **fully glycosylated form (~24 kDa)**, the **mature form (~22 kDa),** and the **immature/non-glycosylated form (~18 kDa),** as indicated. The red box highlights the condition in which all three PMP22 isoforms are simultaneously detected. **B).** PMP22 immunoreactive bands corresponding to the glycosylated form (24 kDa), the mature form (22 kDa), and the non-glycosylated immature form (18 kDa) were quantified by densitometry. Band intensities are expressed in arbitrary units (a.u.) after background subtraction. For each sample, the relative contribution of each isoform is indicated as a percentage of total PMP22 signal (sum = 100%). Bands not visually detectable on the blot were considered absent and assigned a value of 0. Data are shown for individual mice from WT, 5% dextrose–treated C61, and 0.3 mg/kg siRNA PMP22-SQ NP–treated C61 groups. Each Western blot was quantified independently, and the resulting values were subsequently pooled for group comparison.

Morphological and ultrastructural recovery after siRNA PMP22-SQ NPs therapy

Morphometric analyses of sciatic nerves were performed to correlate functional recovery with structural remodeling of myelinated fibers (Figure 6A). g-ratio quantification showed physiological values in WT mice (0.669 ± 0.234), whereas dextrose-treated C61 mice exhibited significantly lower g-ratio values (0.569 ± 0.327), reflecting altered axon–myelin relationships characteristic of dysmyelination rather than physiological myelination. Treatment with siRNA PMP22-SQ NPs at 1.5 mg/kg resulted in g-ratio values partially overlapping with those of dextrose-treated C61 mice (0.560 ± 0.286), indicating limited structural correction.

In contrast, treatment at the lower dose (0.3 mg/kg) resulted in a markedly lower mean g-ratio value (0.359 ± 0.275), reflecting the presence of small-caliber axons surrounded by relatively thick and compact myelin, as observed in the histological sections (Figure 6A-B). Importantly, this pronounced leftward shift of the g-ratio distribution toward lower values indicates substantial axon-myelin remodeling consistent with active or preferential remyelination, rather than complete normalization toward the WT state. Because g-ratio measurements were derived from a large number of individual fibers but a limited number of animals (n = 3 per group), these morphometric findings should be interpreted with caution and primarily reflect intra-nerve structural remodeling rather than inter-animal variability.

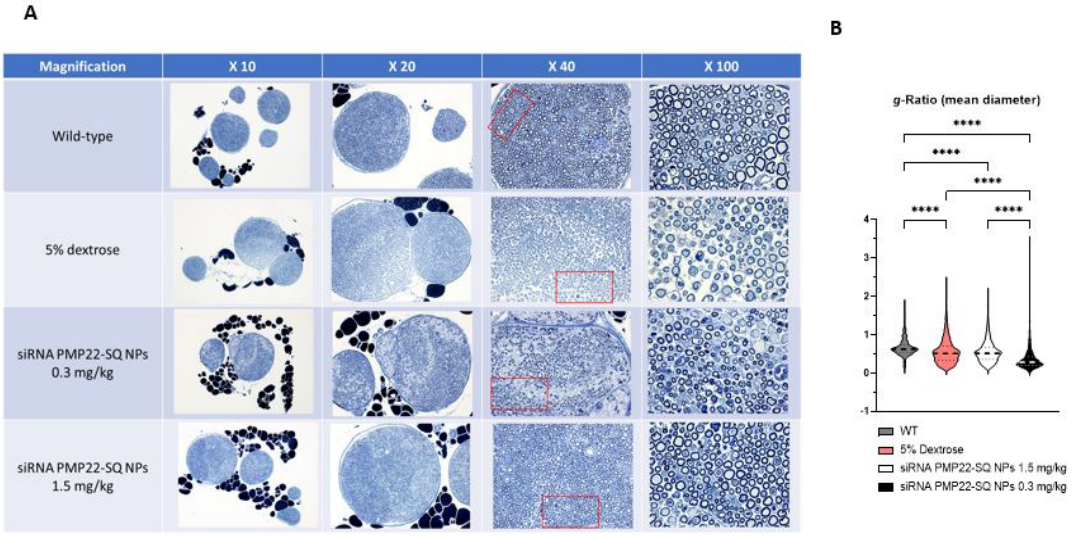

Figure 6: Morphometric analysis of sciatic nerves in C61 mice treated with siRNA PMP22-SQ nanoparticles. **(A)** Representative toluidine blue–stained semi-thin sections of sciatic nerves from WT mice, C61 mice treated with vehicle (5% dextrose), and C61 mice treated with siRNA PMP22-SQ NPs at 1.5 mg/kg or 0.3 mg/kg (n = 3 mice per group). Dextrose-treated C61 nerves display marked dysmyelination and irregular axonal calibers, whereas siRNA PMP22-SQ NP treatment is associated with improved fiber organization and myelin compaction, more pronounced at 0.3 mg/kg than at 1.5 mg/kg. **(B)** g-ratio analysis revealed physiological values in WT mice, reduced g-ratio values in dextrose-treated C61 mice, and no significant change at 1.5 mg/kg, whereas treatment at 0.3 mg/kg induced a significant decrease in mean g-ratio (n = 3 mice per group). Statistical analysis was performed using the Kruskal–Wallis test followed by Dunn's post hoc multiple-comparisons test.

Systemic safety profile of siRNA PMP22-SQ nanoparticles

Serum biochemical parameters were analyzed in C61 mice treated with siRNA PMP22-SQ NPs at cumulative doses of 1.5 mg/kg (three cycles) or 0.3 mg/kg (two cycles) and compared to age matched wild-type and 5% dextrose treated controls (Figure 7).

At the 1.5 mg/kg dose, a moderate increase in total cholesterol and HDL levels was observed after treatment, whereas LDL, triglycerides, and other biochemical parameters remained within the normal range (Figure 7A). This lipid profile modification is likely related to the interaction between squalene nanoparticles and circulating lipoproteins, particularly HDL, which are predominant in mice. Such interactions between squalene-based NPs and HDL/LDL fractions have been previously reported [20]. No such changes were detected in mice treated with the fivefold lower dose (0.3 mg/kg cumulative), suggesting that these lipid variations are dose-dependent and reflect the physiological interaction of the nanoparticles rather than a toxic effect [2].

All other serum parameters, including liver and kidney biomarkers (ALT, AST, urea, creatinine), remained within the normal physiological range, indicating good systemic tolerance to siRNA PMP22-SQ treatment at both doses.

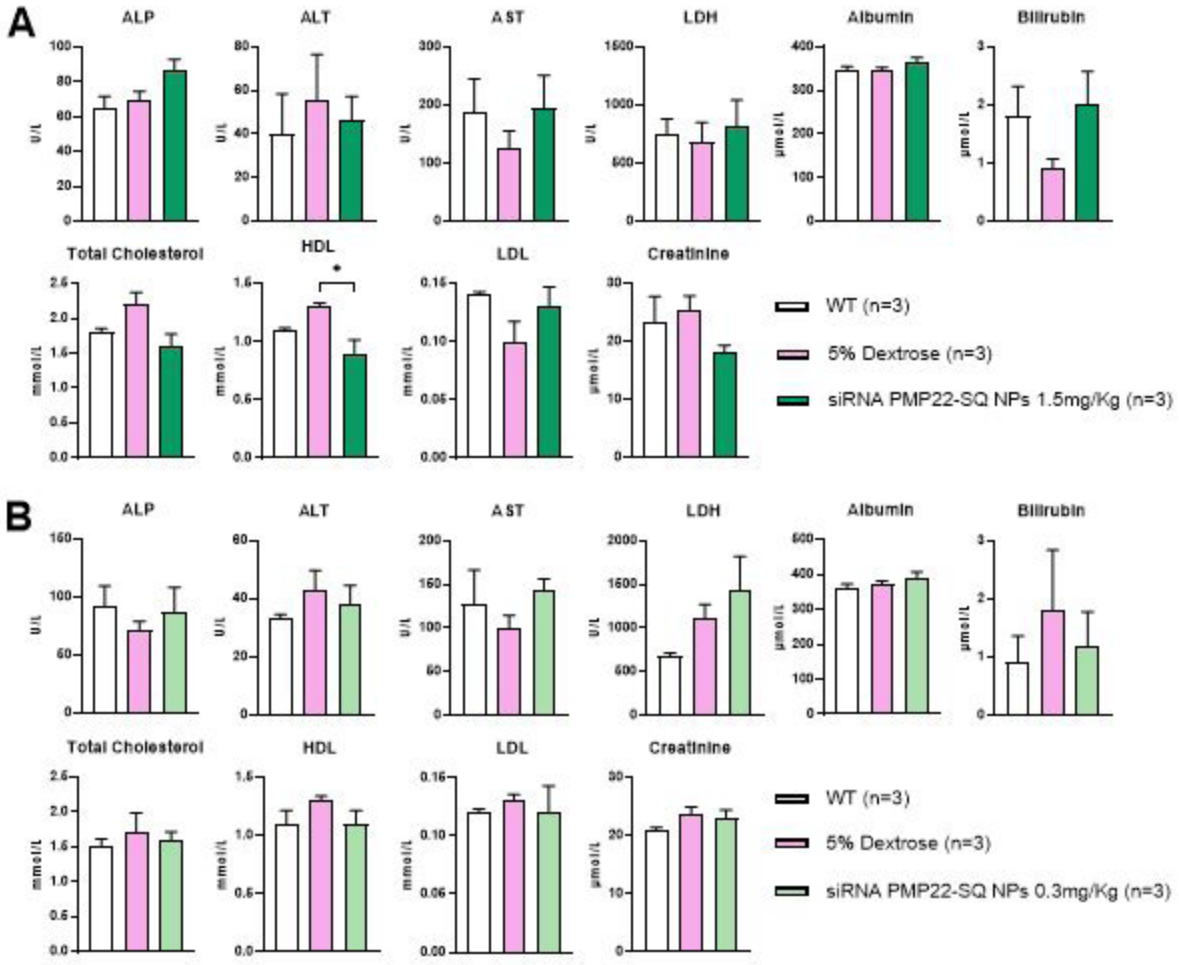

Figure 7: Serum biomarker analysis in C61 mice treated with siRNA PMP22-SQ nanoparticles. (A) Serum biochemical parameters were measured in C61 mice after repeated intravenous administration of siRNA PMP22-SQ nanoparticles at a cumulative dose of 1.5 mg/kg (three treatment cycles) or **(B)** 0.3 mg/kg (two treatment cycles). For each treatment condition, age matched wildtype (WT) and 5% dextrose treated C61 mice were used as controls. Note that WT control groups differed in age, corresponding to the age of the treated C61 mice: one month old WT for the 1.5 mg/kg series and two month,old WT for the 0.3 mg/kg series. Data are expressed as mean ± SEM.* $p < 0.05$ indicates a statistically significant difference between siRNA PMP22-SQ NP treated and 5% dextrosetreated C61 groups (one-way ANOVA followed by Tukey's post hoc test).

Histopathological evaluation of major organs

Histopathological analyses were performed on paraffin embedded sections of brain, spinal cord, sciatic nerve, liver, kidney, heart, and spleen from WT, 5% dextrose treated, and siRNA PMP22-SQ NP–treated C61 mice at the end of the treatment period. Hematoxylin eosin staining revealed normal tissue architecture in all examined organs (Figure 8).

In the central nervous system (brain and spinal cord), no signs of inflammation, gliosis, or structural alterations were detected in any group. In sciatic nerves from C61 mice, mild variability in fiber organization was observed, consistent with the underlying CMT1A phenotype, whereas nerves from siRNA PMP22-SQ-treated animals displayed preserved fascicular architecture without overt structural abnormalities. Semi-thin morphological examination of sciatic nerves revealed no detectable signs of toxicity in either wild-type or siRNA PMP22-SQ treated C61 mice. Myelinated fiber profiles and myelin thickness appeared preserved, without evidence of inflammatory infiltrates (Figure 8A-8B).

In peripheral organs (liver, kidney, heart, and spleen), tissue morphology was preserved, with no necrosis, fibrosis, or vascular congestion detected after repeated siRNA PMP22-SQ NP administrations at either 1.5 mg/kg (three cycles) (Figure 6A) or 0.3 mg/kg (two cycles) (Figure 8B). Hepatocytes, renal glomeruli, cardiac fibers, and splenic architecture appeared normal and comparable to WT and vehicle (5% dextrose) controls. These findings indicate that siRNA PMP22-SQ NPs are systemically well tolerated and do not induce detectable histopathological changes in major organs.

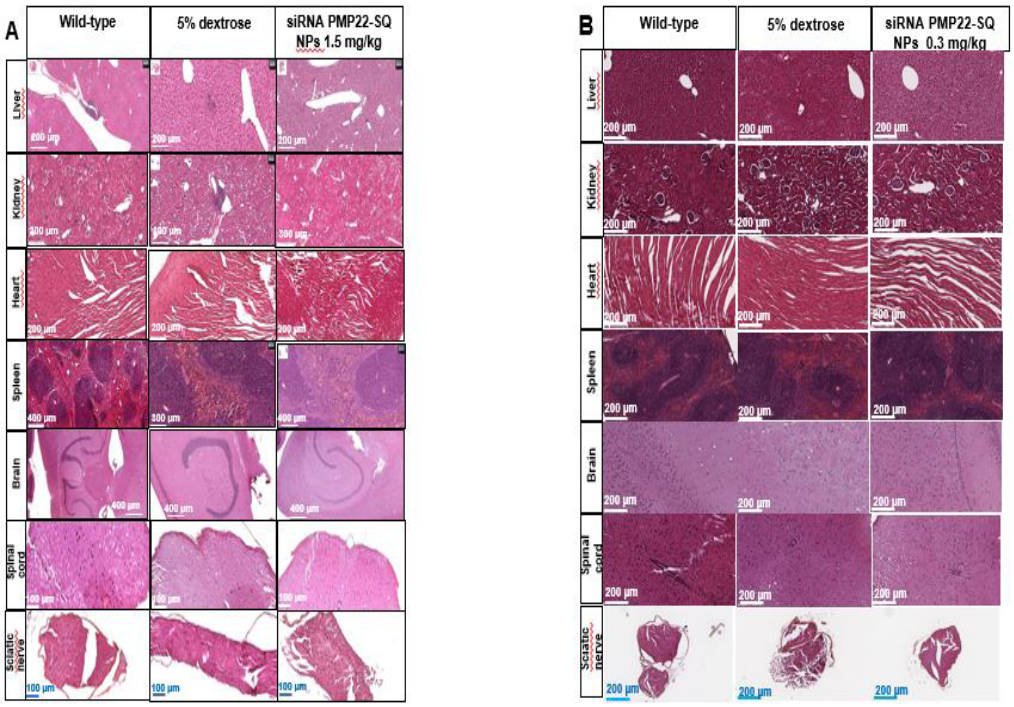

Figure 8: Histopathological evaluation of organs following siRNA PMP22-SQ nanoparticles treatment. Representative hematoxylin eosin (H&E) stained sections of brain, spinal cord, sciatic nerve, liver, kidney, heart, and spleen from WT, 5% dextrose treated, and siRNA PMP22-SQ NPs treated C61 mice. (**A)** Mice treated with 1.5 mg/kg (three treatment cycles, left panels). (**B)** Mice treated with 0.3 mg/kg (two treatment cycles, right panels). No histological abnormalities or inflammatory infiltrates were observed in any organ following siRNA PMP22-SQ NPs administration compared to WT and vehicle controls. The overall tissue architecture was preserved, confirming the good systemic tolerability of the treatment. Scale bars are provided for each histological section.

Discussion

Our findings demonstrate that a short treatment with siRNA PMP22-SQ nanoparticles induces long-lasting therapeutic effects in CMT1A mice. Beneficial effects were observed at both functional and morphological levels and persisted for several months after the last injection. Importantly, these conclusions are based on concordant behavioral, electrophysiological, and morphological readouts obtained in the same experimental cohorts, supporting the robustness of the observed therapeutic benefit.

Remarkably, a very low cumulative dose (0.3 mg/kg total) was sufficient to induce significant improvements in motor performance, nerve conduction, and myelin morphology. At the molecular level, a marked reduction of the aberrant 22 kDa and 18 kDa PMP22 species was observed in two out of three treated mice, whereas the 24 kDa band persisted. This higher molecular weight band most likely corresponds to the fully glycosylated, mature PMP22 protein. Its persistence suggests partial rather than complete suppression of PMP22 expression, with retention of stable or membrane- integrated glycosylated forms that are less sensitive to siRNA-mediated degradation. Consistent with this interpretation, PMP22 is typically detected as multiple immunoreactive species corresponding to immature non-glycosylated and glycosylated forms that accumulate due to proteostasis and trafficking defects in CMT1A models [2, 21]. Thus, the selective reduction of aberrant PMP22 species observed here is consistent with partial restoration of PMP22 proteostasis rather than global protein depletion. The persistence of the therapeutic effect may be related to the long half-life of myelin proteins and the slow turnover of Schwann cells in adult peripheral nerves [22]. Although PMP22 levels were not continuously suppressed, transient normalization may be sufficient to trigger durable structural reorganization. Once compact myelin is restored, newly formed myelin sheaths may remain stable for extended periods in the absence of further treatment, consistent with the sustained functional improvement observed after treatment cessation. Interestingly, treatment with siRNA PMP22-SQ NPs at the lower cumulative dose (0.3 mg/kg) resulted in a marked decrease in mean g-ratio compared with both untreated C61 mice and the higher-dose group. This shift most likely reflects preferential remyelination of small-caliber axons, leading to relatively thick and compact myelin sheaths and consequently lower g-ratio values. Such a pattern is commonly associated with active remyelination rather than pathological hypermyelination, particularly in contexts where Schwann cells re-engage myelination programs. In contrast, the higher dose improved functional outcomes without inducing comparable structural remodeling, suggesting a non-linear dose–response relationship. Importantly, although g-ratio analysis included a large number of individual fibers, the number of animals per group was limited, and individual fibers cannot be considered independent biological replicates. Therefore, these morphometric data primarily reflect intra-nerve structural remodeling and should be interpreted with caution with respect to inter-animal variability, in accordance with ARRIVE recommendations. The observation that the lower dose was more effective than the higher dose suggests the existence of a narrow therapeutic window for siRNA PMP22-SQ NPs treatment. One plausible explanation is that excessive siRNAi delivery may saturate components of the endogenous RNA interference machinery, such as AGO2, thereby reducing productive RISC loading, and silencing efficiency [23]. In addition, high nanoparticle loads may strain intracellular trafficking pathways, diverting material toward non-productive endosomal compartments and limiting cytosolic availability [24]. Given that only a small fraction of internalized siRNA typically reaches the cytosol, increasing the administered dose beyond an optimal threshold does not necessarily enhance target knockdown. Furthermore, Schwann cells with slow turnover and robust homeostatic mechanisms may adapt to persistent target suppression, limiting incremental benefit. Similar saturation and adaptation phenomena have been reported for lipid- or cholesterol-conjugated siRNA [25-28].

Peripheral nerve myelination in mice continues to mature beyond the early postnatal period, with significant metabolic and structural remodeling occurring after weaning [29]. This late maturation phase, around one month of age, represents a stage at which myelin sheaths are largely established yet remain sufficiently plastic to benefit from therapeutic interventions that normalize PMP22 levels. Schwann cells also retain a notable capacity for myelin remodeling in young adulthood, enabling durable correction once healthier myelin has been re-established [30]. Consistent with this, a single treatment cycle administered at two months of age was sufficient to induce a long-lasting functional remission exceeding 100 days. While the present study was not designed to directly compare developmental stages, these observations suggest that therapeutic intervention during this window may favor durable stabilization of myelin architecture. In contrast to PXT3003, which requires chronic daily administration to maintain efficacy, siRNA PMP22-SQ NPs achieved prolonged benefit following a short treatment cycle, highlighting their potential as a durable and less burdensome therapeutic strategy. Nonetheless, direct comparisons between pharmacological and RNA-based approaches should be interpreted cautiously, as mechanisms of action and dosing paradigms differ substantially.

Conclusion

Altogether, these data demonstrate that low-dose systemic administration of siRNA PMP22-SQ nanoparticles effectively improves nerve function, including motor performance, and

promotes structural remodeling in a severe CMT1A mouse model. Although the number of animals per group was limited, the consistency of functional, molecular, and morphological outcomes across independent readouts strengthens the robustness of the conclusions. Collectively, these findings suggest that siRNA PMP22-SQ nanoparticles induce a qualitative reprogramming of Schwann cell myelination toward a more physiological state, supporting durable nerve repair rather than transient molecular compensation.

Data availability: Data are available upon request.

Acknowledgements: Authors thank the team of the animal core facility of BioMedTech Facilities INSERM US36 | CNRS UMS2009.

Author contributions: S.B. designed, performed the experiments and contribute to writing the manuscript. F. P, and E-G. B are involved in histological studies and morphometric analysis. L.M. is the PI of the study, she supervised, designed the study and wrote the manuscript.

Funding Source

This work was supported by the "SATT Paris Saclay", program Maturation siCMT.

Conflict of interests: The authors declare that no conflict of interest exists.

Declaration of generative AI and AI-assisted technologies in the manuscript preparation process. During the preparation of this manuscript, the authors used AI-assisted tools to improve language clarity and readability. The authors reviewed and edited all content and take full responsibility for the scientific content of the article.

References

1. Timmerman V, Nelis E, Van Hul W, Nieuwenhuijsen BW, Chen KL, et al. (1992). The peripheral myelin protein gene PMP-22 is contained within the Charcot-Marie-Tooth disease type 1A duplication. Nature Genetics. 1: 171-175.
2. Prior R, Silva A, Vangansewinkel T, Idkowiak J, Tharkeshwar AK, et al. (2024). PMP22 duplication dysregulates lipid homeostasis and plasma membrane organization in developing human Schwann cells. Brain. 147: 3113-3130.
3. Attarian S, Young P, Brannagan TH, Adams D, Van Damme P, et al. (2021). A double-blind, placebo-controlled, randomized trial of PXT3003 for the treatment of Charcot-Marie-Tooth type 1A. Orphanet Journal of Rare Diseases. 16: 433-433.
4. Boutary S, Caillaud M, El Madani M, Vallat JM, Loisel-Duwattez J, et al. (2021). Squalenoyl siRNA PMP22 nanoparticles are effective in treating mouse models of Charcot-Marie-Tooth disease type 1 A. Commun Biol. 4: 317.
5. Espallergues J, Cadiet J, Souab F, Choquet O, Swisser F, et al. (2025). Perineural delivery of AAV2/9 in non-human primates is a safe and efficient route for gene therapy in Charcot-Marie-Tooth diseases. Mol Ther Methods Clin Dev. 33: 101548.
6. Gautier B, Hajjar H, Soares S, Berthelot J, Deck M, et al. (2021). AAV2/9-mediated silencing of PMP22 prevents the development of pathological features in a rat model of Charcot-Marie-Tooth disease 1A. Nat Commun. 12: 2356.
7. Serfecz J, Bazick H, Al Salihi MO, Turner P, Fields C, et al. (2019). Downregulation of the human peripheral myelin protein 22 gene by miR-29a in cellular models of Charcot-Marie-Tooth disease. Gene Ther. 26: 455-464.
8. Stavrou M, Kagiava A, Choudury SG, Jennings MJ, Wallace LM, et al. (2022). A translatable RNAi-driven gene therapy silences PMP22/Pmp22 genes and improves neuropathy in CMT1A mice. J Clin Invest. 132.
9. Boutary S, Khalaf G, Landesman Y, Madani ME, Desmaële D, et al. (2025). Therapeutic potential of siRNA PMP22-SQ nanoparticles for Charcot-Marie-Tooth 1A neuropathy in rodents and non-human primates. Int J Pharm. 671: 125234.
10. Boutary S, Khalaf G, Caillaud M, Desmaële D, Yesylevskyy S, et al. (2023). Optimizing Structure and Activity of the Squalenoyl-siRNA Nanoparticles. Journal of Clinical Toxicology. 13: 1000530.
11. Caillaud M, El Madani M, Massaad-Massade L. (2020). Small interfering RNA from the lab discovery to patients' recovery. J Control Release. 321: 616-628.
12. Massaad-Massade L, Boutary S, Caillaud M, Gracia C, Parola B, et al. (2018). New Formulation for the Delivery of Oligonucleotides Using "Clickable" siRNA-Polyisoprenoid-Conjugated Nanoparticles: Application to Cancers Harboring Fusion Oncogenes. Bioconjug Chem. 29: 1961-1972.
13. Ali HM, Maksimenko A, Urbinati G, Chapuis H, Raouane M, et al. (2014). Effects of silencing the RET/PTC1 oncogene in papillary thyroid carcinoma by siRNA-squalene nanoparticles with and without fusogenic companion GALA-cholesterol. Thyroid. 24: 327-338.
14. Urbinati G, Ali HM, Rousseau Q, Chapuis H, Desmaële D, et al. (2015). Antineoplastic Effects of siRNA against TMPRSS2-ERG Junction Oncogene in Prostate Cancer. PLoS One. 10: e0125277.
15. Fledrich R, Stassart RM, Sereda MW. (2012). Murine therapeutic models for Charcot-Marie-Tooth (CMT) disease. Br Med Bull. 102: 89-113.
16. Huxley C, Passage E, Manson A, Putzu G, Figarella-Branger D, et al. (1996). Construction of a mouse model of Charcot-Marie-Tooth disease type 1A by pronuclear injection of human YAC DNA. Hum Mol Genet. 5: 563-569.
17. Notterpek L, Ryan MC, Tobler AR, Shooter EM, Snipes GJ. (1999). PMP22 accumulation in aggresomes: Implications for CMT1A pathology. J Neurosci. 19: 3378-3387.
18. Pareek S, Notterpek L, Snipes GJ, Naef R, Sossin W, et al. (1997). Neurons promote the translocation of peripheral myelin protein 22 into myelin. J Neurosci. 17: 7754-7762.
19. Ryan MC, Shooter EM, Notterpek L. (2002). Aggresome formation in neuropathy models based on peripheral myelin protein 22 mutations. Neurobiology of Disease 10: 109-118.
20. Caillaud M, Gobeaux F, Hémadi M, Boutary S, Guenoun P, et al. (2021). Supramolecular organization and biological interaction of squalenoyl siRNA nanoparticles. Int J Pharm. 609: 121117.

21. Moore SM, Gawron J, Stevens M, Marziali LN, Buys ES, et al. (2024). Pharmacologically increasing cGMP improves proteostasis and reduces neuropathy in mouse models of CMT1. Cell Mol Life Sci. 81: 434.

22. Snipes GJ, Suter U, Welcher AA, Shooter EM. (1992). Characterization of a novel peripheral nervous system myelin protein (PMP22/SR13). Journal of Cell Biology. 117: 225-238.

23. Motamedi H, Ari MM, Alvandi A, Abiri R. (2024). Principle, application and challenges of development siRNA-based therapeutics against bacterial and viral infections: a comprehensive review. Front Microbiol. 15: 1393646.

24. Åberg C. (2021). Kinetics of nanoparticle uptake into and distribution in human cells. Nanoscale Adv. 3: 2196-2212.

25. Ebenezer O, Oyebamiji AK, Olanlokun JO, Tuszynski JA, Wong GK. (2025). Recent Update on siRNA Therapeutics. Int J Mol Sci. 26: 3456.

26. Hu B, Zhong L, Weng Y, Peng L, Huang Y, et al. (2020). Therapeutic siRNA: state of the art. Signal Transduct Target Ther. 5: 101.

27. Lorenz C, Hadwiger P, John M, Vornlocher HP, Unverzagt C. (2004). Steroid and lipid conjugates of siRNAs enhance cellular uptake. Bioorganic & Medicinal Chemistry Letters. 14: 4975-4977.

28. Rozema DB, Lewis DL, Wakefield DH, Wong SC, Klein JJ, et al. (2007). Dynamic PolyConjugates for targeted in vivo delivery of siRNA to hepatocytes. Proc Natl Acad Sci. 104: 12982-12987.

29. Fledrich R, Abdelaal T, Rasch L, Bansal V, Schütza V, Brügger B, et al. (2018). Targeting myelin lipid metabolism as a potential therapeutic strategy in a model of CMT1A neuropathy. Nat Commun. 9: 3025.

30. Jessen KR, Mirsky R. (2005). The origin and development of glial cells in peripheral nerves. Nat Rev Neurosci. 6: 671-682.